Determining the Proper Mix of Incinerator Bottom Ash for Floor Tile Manufacturing

Deng-Fong Lin
I-Shou University
Kuo-Liang Lin (kllin@isu.edu.tw)
I-Shou University https://orcid.org/0000-0002-5336-9309
Show-Ing Shieh
Shu-Te University
Chia-Wen Chen
I-Shou University

Research Article

Keywords: incinerator bottom ash, ceramic floor tiles, SEM, NMR, replacement level

Posted Date: March 30th, 2021

DOI: https://doi.org/10.21203/rs.3.rs-298743/v1

Abstract

Since 2003, researchers have attempted to reuse incinerator bottom ash (IBA), the residual from incinerating municipal solid waste, for ceramic production. This study focused on investigating proper IBA replacement level for manufacturing interior and exterior floor tiles. Firstly, raw materials of clay and IBA underwent SEM, EDS, and TCLP tests to determine their chemical contents. Six sets of specimens with different replacement levels of IBA (0%, 5%, 10%, 15%, 20%, and 30%) were then prepared. The specimens were calcined at 1000℃, 1050℃,1100℃, and 1150℃ and subsequently put through a series of mechanical tests to compare their performance. NMR (nuclear magnetic resonance spectroscopy) were also used to determining the organic compound structure after each specimens' crystallization. Research results showed that proper mix of IBA up to 20% could result in quality tiles complying with specifications for interior and exterior flooring applications at certain kiln temperatures, while the specimens with 30% IBA failed to meet either bending strength or size shrinkage requirement at all kiln temperatures, and could not deliver a satisfactory result no matter what.

1. Introduction

The Taiwan Environmental Protection Administration (TEPA) has launched a series of municipal solid waste incinerator construction projects to offer one incinerator for each local government starting from 1991. As the incinerators start to function, past problems caused by solid waste disposal has been resolved while incineration becomes the primary method for treating municipal solid waste. However, the increasing amount of incinerator bottom ash (more than 100 million tons per year and increasing each year) has raised new environmental issues. Landfills have been the number one option for incinerator bottom ash but is not deemed as a sustainable solution. Many researchers have been studying recycle and reuse of incinerator bottom ash (IBA) so that the ultimate sustainable goal of zero-waste can be achieved someday (EPA 2020). Incinerator bottom ash is a light-weighted porous material with high water-absorbing characteristic (Balapour et al. 2020). The product made with bottom ash tend to be brittle and easy to wear (Filipponi et Al. 2003). The main oxides present in most bottom ash are SiO2, CaO and Al2O3, with others such as Fe2O3, Na2O, MgO, SO3, Cl−, P2O5, ZnO and CuO present in smaller amounts (Lynn et al. 2017).

During the incineration, bottom ash goes through a process of carbonation and the degree of carbonation decreased as the size increased, which in turn corresponded to decreasing total Ca content and portlandite phase (Lin et al. 2015). Many have suggested that significant quantities of bottom ash with fine grain size, typically less than 4 mm, is limited in reuse options. However, a British study concluded that the fine fractions of problematic incinerated bottom ash can be transformed into an inert material suitable for the production of hard, dense ceramics, no matter the ash is obtained from dry discharge system or a wet discharge system based on proper incineration process (Bourtsalas 2015).

In 2003, Cheeseman et al. reported a successful ceramic processing of incinerator bottom ash. Attempting sintering milled incinerator bottom ash at 1110 ◦C, they produced ceramics with densities

between 2.43 and 2.64 g/cm3 and major crystalline phases of wollastonite (CaSiO3) and diopside (CaMgSi2O6), but no replacement level has been revealed (Cheeseman et al. 2003). Two other studies then suggested replace percentage for the IBA for making ceramic products. In 2012, an Italian study reported a remarkable amount (60 wt%) of alternative raw material from post-treated municipal solid waste incinerator and 40 wt% of refractory clay (Schabbach et al. 2012). Sintering range between 1190–1240 ◦C, the study demonstrated specimens having low water absorption and high crystallinity with bending strength higher than 40 MPa. In 2016, on the other hand, a study from Ireland made a more conservative statement and suggested that bottom ash replacement levels have to be below 20% in order to provide adequate compression and tensile strengths with density and absorption at satisfactory levels (Holms et al. 2016).

To investigate the discrepancy of the replacement level of IBA in previous studies, specimens were made with six different mixes of replacement levels of IBA, namely 0%, 5%, 10%, 15%, 20%, 30%. These specimens were calcined at four different temperatures (1000℃, 1050℃,1100℃, and 1150℃). Basic properties such as specific gravity, unit weight, porosity, specific surface area, and sieve analysis of the raw materials were first examined and the chemical contents of clay and IBA were identified with SEM, EDS, and TCLP. After the specimens were calcined, they were put through a series of mechanical tests to compare their performance. NMR (nuclear magnetic resonance spectroscopy) were also used to determining the organic compound structure after each specimens' crystallization through kilning.

2. Materials

2.1 Basic properties of the raw materials

The clay used in the study was obtained from a local kiln plant in Kaohsiung, and incinerator bottom ash (IBA) was acquired from a municipal waste incineration plant near Taichung City. Table 1 shows the basic properties of clay and IBA. Because the IBA was obtained from incinerated refuses at high melting temperature, lots of pores were observed on its surface. The specific gravity of the IBA was smaller than that of the clay, as shown in the Table 1. Figure 1 shows the sieve analysis results that reveals the particle size distributions of both clay and IBA. Particle sizes of IBA fell between 0.03 and 0.3mm with an accumulative amount of 83.63%. Particle sizes of our clay were uniformly distributed and had an accumulative amount of 55.63% smaller than 0.075mm. Based on the sieve analysis, IBA were coarser than clay.

Table 1 Basic Properties of Clay and IBA

	Clay	IBA
Specific gravity	2.64	2.21
Unit weight (kg/m^3)	1243.58	1039
Pore ratio (%)	60.12	63.05
Specific surface area (cm^2/g)	2583.77	1296.32

2.2 SEM ▯ EDS

Figure 2 shows the images of SEM enlarged at 5000 times for clay and IBA. As shown in the images, the clay has a smoother surface and its structure appeared to be relatively simple. Because the IBA was obtained from the refuses incinerated at high temperature and the sources of refuses were complicated, the structure of interior crystals for IBA was more complicated than that of the clay. Table 2 shows the EDS results of the clay and IBA. As seen in the table, the largest amounts of chemical elements for clay and IBA were Si and Ca with the amount of 27.9% and 18.9%, respectively.

Table 2 EDS results of the clay and IBA

Element	C	O	Na	Mg	Al	Si	S	Cl	K	Ca	Fe	Zn	Br	Zr
Clay(%)	-	49.9	1.19	1.05	9.46	27.9	-	-	2.64	1.37	6.49	-	-	-
IBA(%)	18.5	40.9	-	-	-	3.44	1.37	2.19	-	18.9	-	2.52	4.46	7.77

2.4 TCLP test

To recycle the IBA as construction material, the TCLP test result of the IBA must meet the requirement of the hazardous industrial waste standard. Table 3 shows the TCLP test results for IBA. The highest amount of heavy metal detected for IBA was Cu, followed by Ba and Cd. All other heavy metals were not detectable for IBA. It suggests that the IBA is suitable to be recycled.

Table 3 TCLP test results for IBA

Element	As	Pb	Cu	Cd	Cr	Hg	Cr^{6+}	Se	Ba
IBA(mg/L)	ND	ND	1.65	<0.100	ND	ND	ND	ND	0.641
Standard	≦0.4	≦4.0	≦12.0	≦4.0	≦0.8	≦0.016	≦0.2	≦0.8	≦10.0

3. Results And Discussion

Specimens with 5 different IBA replacement amount of 0%, 5%,10%, 15%, and 20%(wt) were prepared. Before the specimens were made, the raw materials went through Atterberg limits to derive their plasticity limits so that proper mixing water quantities could be determined. In the process of fabrication, proper compositions of clay, IBA were uniformly mixed in a shaft clay mixer first, and the mixtures were kneaded with a de-airing vacuum pug mill to reduce extra interior pores. Next, the well-kneaded mixtures were placed in a mold with the size of 12 * 6*1 cm^3 and compressed by a pressing machine with a normal pressure of 34.32 ± 0.5 MPa to produce the specimens. Specimen were then kilned at 4 different temperatures, 1000℃,1050℃,1100℃, and 1150℃. Based on the mixture and kilned temperatures, 20 sets of specimens were made. Each set of specimens had 30 tile samples ready for a series of tests, including shrinkage, weight loss on ignition, specific gravity, water absorption, bending strength, wear resistance, SEM, EDS, XRD, and NMR..

3.1 Atterberg limits

The plastic limits obtained from plastic limit tests for different mix designs were used to study the effects of the various IBA replacements on the amount of water applied at each mix design. Figure 3 shows the results of the plastic limit at different amounts of IBA replacement. Because the IBA was characterized as

porous material with high water absorption. As shown in the figure, the plastic limits increased first and then decreased with the increasing amount of the IBA replacement. When applied IBA to the floor tiles, the water used in the mixing process was increased. Moreover, IBA was characterized as hydrophobic non-plastic material. After the amount of IBA replacement reached to 10%, the plastic limit reduced with the increasing amount of the IBA replacement.

3.1 Shrinkage

Figure 4 shows results of the shrinkage for floor tiles contained with different amounts of IBA replacement firing at various kiln temperatures. A study by (Valle-Zermeño et al 2016) suggested that when the particle size was small, the diffusion became better and the neck effect grew fast leading to a better compaction for ceramic tiles. Because the particle sizes of IBA were larger than that of clay, the particles were hard to mixed uniformly inside the structure of floor tiles. Hence, the shrinkage of the floor tiles reduced with the increasing amount of the IBA replacement within the kiln temperature of 1000-1100^{o}C. Moreover, Figure 5 shows the shrinkage and expansion of the floor tile specimens at different kiln temperature. When the kiln temperature increased, the pores among particles were pushed and compacted by the thermal force driven from heat in the floor tile specimens. The shrinkage of the tile specimens reduced first and then expanded with the increasing of the kiln temperature, as shown in the figure 5. The highest shrinkage of the floor tile specimens was 5.25% at the initial stage of firing temperature of 1000^{o}C. When the kiln temperature reached to 1100^{o}C, the highest shrinkage of the tile specimens was observed. It suggests that the interior of the floor tile specimens was completely compacted. Finally, as the kiln temperature increased 50^{o}C more, melting of the tile body was noticed and entrapped air was wrapped by glass film. As a result, the tile body was expanded, which comply with the pioneering study at Imperial College (Cheesman et al. 2003). Another study by (Bernd and Carl 1997) suggested that the expansion of tile body was reduced if the tile specimens contained with large amount of CaO. It was also possible that the shrinkage of tile specimens could be turned from negative to positive with the amount of IBA replacement increased at kiln temperature of 1150^{o}Cn (Bijen 1986).

3.2 Weight loss on ignition

Figure 5 shows results of the weight loss on ignition for floor tiles contained with different amounts of IBA replacement firing at various kiln temperatures. Because IBA contained with large amount of organic and non-organic matters and heavy metals in which were easily burned or become fugitive emissions at high kiln temperature. The weight loss on ignition of floor tile specimens increased with increasing amount of IBA replacement. Although the weight loss on ignition increased with the increasing of the kiln temperature, the increment of weight loss on ignition became less with the increasing amount of IBA replacement.

3.3 Specific gravity

Figure 6 shows results of the specific gravity for floor tiles contained with different amounts of IBA replacement firing at various kiln temperatures. Because the IBA contained with $CaCO_3$ leading to an increase of pore volume inside the tile body, the specific gravity of the floor tile specimens reduced with the increasing amount of IBA replacement within the kiln temperature of 1000-1100^oC. As the kiln temperature reached to 1150^oC, the specific gravity increased with the increasing amount of IBA replacement. The high kiln temperature could result in a rearranging of particle in the interior structure of the floor tile specimens, producing compaction of tile body, and pore volume circularized and vanished. The specific gravity of the tile specimens reduced with the increasing kiln temperature within the kiln temperature of 1000-1100^oC. At kiln temperature of 1100^oC, the pores in the tile body were circularized and vanished leading to a more compact interior structure of floor tile and apparent increase of specific gravity was observed. However, as the kiln temperature reached to 1150^oC, the tile body became to melt and foam and pores were produced in the interior of specimens leading to a decrease on the specific gravity.

3.4 Water absorption

Figure 7 shows results of the water absorption for floor tiles contained with different amounts of IBA replacement firing at various kiln temperatures. Bernd and Carl [1997] pointed out that the carbonates in the tile body could increase the water absorption of tile specimens. IBA contained with large amount of $CaCO_3$ in which characterized as carbonate. The water absorption of floor tile specimens increased with increasing amount of IBA replacement, as shown in the Figure 7. Moreover, pores in the interior structure of tile specimens were gradually circularized and vanished driven by the thermal force from heat. As a result, the interior structure became compact. The water absorption of floor tile specimens contained with IBA replacement reduced with the increasing of kiln temperature. When the kiln temperature reached to 1150^oC, the surface of the floor tile specimens became shiny and water was hard to penetrate into tile specimens. Hence, the water absorption for floor tile specimens firing at kiln temperature of 1150^oC was close to zero, as also shown in Figure 7 and Figure 8.

3.5 Bending strength

Figure 9 shows results of the bending strength for floor tiles contained with different amounts of IBA replacement firing at various kiln temperatures. Because IBA was a porous material, the porosity of the floor tile specimens increased with increasing amount of IBA replacement. This increasing of porosity could affect the interior structure of tile specimens. The bending strength of floor tile specimens reduced with increasing amount of IBA replacement, as shown in the Figure 9. Moreover, high kiln temperature could reduce pores in the tile specimens leading to a more compact interior structure of floor tile specimens. The bending strength of floor tile specimens containing with IBA replacements increased with increasing kiln temperature within the range of 1000-1100^oC, as shown in the Figure 9. However, when kiln temperature reached to 1150^oC, foam was produced in the tile specimens and the bending strength

of tile specimens reduced, as shown in the Figure 9, while Figure 10 shows the cross section of the tile specimens.

3.6 Wear resistance

Figure 11 shows results of the wear resistance for floor tiles contained with different amounts of IBA replacement firing at various kiln temperatures. Because IBA was a porous material, the compaction of floor tile specimens became less with increasing amount of clay replaced by IBA firing at the same kiln temperature. Hence, the amount of wear for tile specimens increased with increasing amount of IBA replacement. Moreover, the thermal force from heat could produce more compact interior structure for floor tile specimens. The amount of wear for tile specimens reduced with increasing kiln temperature with the range of 1000-1100^{o}C, as shown in the Figure 11. However, when kiln temperature reached to 1150^{o}C, melting of the tile specimens was observed and foam was produced in the tile specimens. Hence, the amount of wear for tile specimens firing at 1150^{o}C was more than that firing at 1100^{o}C, as shown in the Figure 11 and 12.

3.7 SEM analysis

Figures 13 and 14 show SEM images for floor tiles contained with 0 and 20% IBA replacements firing at various kiln temperatures, respectively, while Figures 15 shows SEM images for floor tiles containing different amount of IBA replacements firing at kiln temperature of ***1150^{o}C***. The images were magnified at 5000 times. Because IBA contained with $CaCO_3$ in which decomposed into CaO and CO_2 at high kiln temperature. As a result, pores would be increased by the addition of IBA replacement. The SEM images show that holes in the interior structure of floor tile specimens increased with increasing amount of IBA replacement firing at the same kiln temperature. As stated above, the interior structure of the floor tile specimens became more compact at kiln temperature of 1100^{o}C driven by the thermal force from heat, as shown in the Figure 13 and 14. The pores reduced and strength increased. Hence, the largest bending strength and least amount of wear were obtained for tile specimens firing at kiln temperature of 1100^{o}C. Moreover, when kiln temperature reached to 1150^{o}C and passed over the melting point of tile specimens, the floor tile specimens began to melt and foam was formed with holes produced. Hence, the bending strength of the tile specimens reduced at kiln temperature of 1150^{o}C.

3.8 EDS analysis

Figure16 shows results obtained from EDS analysis for floor tiles contained with different amounts of IBA replacement firing at kiln temperature of 1150^{o}C. The main and trace chemical elements in the floor tile specimens contained with different amount of IBA replacement were O, Mg, Al, Si, K, Ca, and Fe, and C, Na, Ti, and Zr, respectively. The main chemical elements in the floor tile specimens were little affected by kiln temperature. Moreover, there were no apparent differences on main chemical elements for floor tile specimens contained with different amount of IBA replacement as the kiln temperature increased. As stated above, the main chemical element of IBA was Ca and the amount of Si was less in IBA. The

amount of Si in floor tile specimens decreased with increasing amount of IBA replacement firing at the same kiln temperature.

3.9 XRD analysis

Table 4 shows results obtained from XRD analysis for floor tiles contained with different amounts of IBA replacement firing at various kiln temperatures. The main component in floor tile specimens was SiO_2. The IBA contained with $CaCO_3$. When the amount of IBA replacement increased, the amounts of productions of $CaSiO_3$ and $Ca(Al_2Si_2O_8)$ produced from SiO_2 with CaO and Al_2O_3 increased, as shown in the Table 4. As discussed above, the bending strength of floor tile specimens decreased with increasing amount of IBA replacement. It suggests that the amounts of $CaSiO_3$ and $Ca(Al_2Si_2O_8)$ increased with the increasing amount of IBA replacement may lead to a decrease on bending strength of tile specimens. Moreover, the amount of production of $MgSiO_3$ produced from SiO_2 and MgO increased with the increasing kiln temperature resulting in an increase of bending strength of floor tile specimens within the temperature of 1000-1100^oC. However, as the kiln temperature reached to 1150^oC, more amount of $Ca(Al_2Si_2O_8)$ was produced and the bending strength of tile specimens reduced.

Figure 17 shows SEM images for floor tiles contained with 0% IBA replacements firing at kiln temperatures of 1000-1150^oC. The red arrow in the figure pointed to the crystal products of SiO_2 and Al_2O_3 in the interior structure of floor tile specimens. The amount of crystal products reduced with increasing of kiln temperature. It suggests that the tile body structure became compact as the kiln temperature increased. Figure 18 shows SEM images for floor tiles contained with 5-20% of IBA replacement firing at kiln temperature of 1150^oC. When part of clay replaced by IBA, impurities were observed on the images of tile specimens. It suggests from EDS analysis that the impurities were Ca related compounds because IBA contained with large amount of Ca element. The Ca related compounds increased with increasing amount of IBA replacement.

Table 4 XRD analysis for floor tiles

Temperature	IBA %	SiO_2	$AlPO_4$	$CaSiO_3$	$MgSiO_3$	$Ca(Al_2Si_2O_8)$	$K(AlSi_3O_8)$
1000°C	0%	54.9	1.2	4.4	16.5	16.3	6.8
	10%	56.4	0.3	7.7	9.0	21.8	4.8
	20%	36.9	0.4	10.2	24.8	20.9	6.8
1050°C	0%	45.8	1.9	10.4	14.1	15.4	12.4
	10%	54.2	0.1	5.8	20.0	17.0	2.9
	20%	55.8	0.7	-	-	43.5	-
1100°C	0%	84.3	2.7	13.0	-	-	-
	10%	52.7	1.2	-	25.0	15.1	6.1
	20%	37.0	1.6	-	41.3	20.1	-
1150°C	0%	65.3	2.0	8.0	15.5	9.2	-
	10%	40.2	1.2	-	-	21.2	10.6
	20%	33.7	1.4	-	-	45.5	19.3

3.10 NMR analysis

Figure19 shows integration result of NMR spectra analysis for floor tiles contained with different amounts of IBA replacement firing at kiln temperature of 1050^{o}C. Q^{x} stands for the location of Si in the tetrahedral structure. Q^{0} is the location of the un-connecting Si atom in the tetrahedral structure with chemical shifts between -68 and -76ppm. Q^{1} is at the location connecting to one Si atom with chemical shifts between -76 and -82ppm. Q^{2} has chemical shifts between -82 and -88ppm. Q^{3} has chemical shifts between -88 and -98ppm. Q^{4} is at the location connecting to four Si atoms with chemical shifts between -98 and -129ppm (He and Hu 2007). The values of Q^{4} after integration decreased with increasing amount of IBA replacement. Because the IBA contained with less amount of Si than that of clay, the amount of silicate became less with insufficient Si atom in the tile specimens. Moreover, the less amount of silicate lead to the decrease of bending strength for tile specimens in which conformed with the results obtained from bending strength tests.

3.11 Quality summary for floor tile

Table 5 shows the quality requirements for ceramic floor tiles contained with IBA and SSA replacements. The qualified rate for bending failure loading decreased with increasing amount of IBA replacement. Because IBA was a material with large porosity, the amount of IBA replacement increased resulted in an increase of porosity for floor tile specimens and reduction on qualified rate for tile specimens. Moreover, the high kiln temperature improved the compaction of floor tile specimens. The qualified rate of bending failure loading for tile specimens increased with increasing kiln temperature. At kiln temperature of 1100^{o}C, the bending failure loadings for floor tile specimens contained with different amount of IBA replacement met the requirement set by the standards. In general, the floor tile specimens contained with different amount of IBA replacement firing at various kiln temperature met the requirement for type III water absorption set by the standards. As for type Ia, Ib, and II water absorption, the qualified rates were improved by increasing kiln temperature. Because the IBA contained with $CaCO_3$ in which decomposed into CaO and CO_2 and formed air bubbles at high kiln temperature, the qualified rate of water absorption decreased with increasing amount of IBA replacement. Table 6 shows the floor tile specimens with different mix designs met the requirements set by the standard. As shown in the table, the tile specimens contained with 5% IBA replacement firing at kiln temperature of 1050-1150^{o}C met the requirements set for the exterior ceramic floor tile standards. Moreover, the same mix design of tile specimens firing at kiln temperature of 1100^{o}C met the requirements for the interior floor tile standards and the high standard of Ib water absorption requirement.

Table 5 Quality compliance summary for all tile specimens

Material		Temperature (℃)	Judgment criteria							
			Interior floor tile		Exterior floor tile		Water absorption(%)			
Clay (%)	IBA (%)		Bending strength	Size shrinkage	Bending strength	Size shrinkage	Ia	Ib	II	III
100	0	1000	●	×	×	×	×	×	×	●
		1050	●	×	●	●	×	×	●	●
		1100	●	×	●	×	×	●	●	●
		1150	●	×	●	●	●	●	●	●
95	5	1000	●	×	×	×	×	×	×	●
		1050	●	×	●	●	×	×	×	●
		1100	●	●	●	●	×	●	●	●
		1150	●	×	●	●	×	●	●	●
90	10	1000	●	×	×	●	×	×	×	●
		1050	●	×	×	×	×	×	×	●
		1100	●	×	●	×	×	×	●	●
		1150	●	×	●	●	●	●	●	●
85	15	1000	×	×	×	●	×	×	×	●
		1050	●	●	×	●	×	×	×	●
		1100	●	×	●	×	×	×	●	●
		1150	●	×	●	●	×	●	●	●
80	20	1000	×	×	×	×	×	×	×	●
		1050	●	●	×	●	×	×	×	●
		1100	●	×	●	×	×	×	●	●
		1150	●	×	●	●	×	●	●	●
70	30	1000	×	●	×	●	×	×	×	●
		1050	×	●	×	●	×	×	×	●
		1100	●	×	●	×	×	×	●	●
		1150	●	×	●	×	●	●	●	●

Table 6 6 Suggested applications for tiles with different IBA replacement

Material		Temperature (°C)	Judgment criteria (Interior floor tile / Exterior floor tile)	Water absorption (Ia Ib II III)
Clay (%)	IBA (%)			
100	0	1050	Exterior floor tile	II III
		1150	Exterior floor tile	Ia Ib II III
95	5	1050	Exterior floor tile	III
		1100	Interior floor tile/ Exterior floor tile	Ib II III
		1150	Exterior floor tile	Ib II III
90	10	1150	Exterior floor tile	Ia Ib II III
85	15	1050	Interior floor tile	III
		1150	Exterior floor tile	Ib II III
80	20	1050	Interior floor tile	III
		1150	Exterior floor tile	Ib II III

4. Conclusion

Our research results showed that proper mix of IBA up to 20% at certain kiln temperature could result in quality tiles complying with all specifications for both interior and exterior flooring applications. However, when IBA was increased to 30%, it failed to meet either bending strength or size shrinkage requirement at all kiln temperatures. We concluded that the maximum replacement level of IBA for ceramic production is 20%. Some other important findings are summarized as following:

1. The shrinkage of floor tile specimens reduced with increasing amount of IBA replacement within the kiln temperature of 1000-1100^{o} When kiln temperature reached to 1150^{o}C, the shrinkage changed from negative to positive with the increasing amount of IBA replacement.
2. Because IBA contained with large amount of $CaCO_3$, the water absorption of floor tile specimens increased with increasing amount of IBA replacement. The water absorption of floor tile specimens contained with IBA replacement reduced with the increasing of kiln temperature. When the kiln temperature reached to 1150^{o}C, the surface of the tile specimens became shiny and water was hard to penetrate into tile specimens. Hence, the water absorption for floor tile specimens firing at kiln temperature of 1150^{o}C was close to zero.
3. Because the porosity of the floor tile specimens increased with increasing amount of IBA replacement, this increasing of porosity could affect the interior structure of tile specimens. The

bending strength of floor tile specimens reduced with increasing amount of IBA replacement. Moreover, high kiln temperature compacted the interior structure of floor tile specimens. The bending strength of floor tile specimens containing with IBA replacements increased with increasing kiln temperature within the range of 1000-1100^{o} However, when kiln temperature reached to 1150^{o}C, foam was produced in the tile specimens and the bending strength of tile specimens reduced.

4. Because IBA was a porous material, the amount of wear for tile specimens increased with increasing amount of IBA replacement. The amount of wear for tile specimens reduced with increasing kiln temperature with the range of 1000-1100^{o} The best resistance to wear for tile specimens was fired at kiln temperature of 1100^{o}C.
5. The SEM images show that pores in the interior structure of floor tile specimens increased with increasing amount of IBA replacement. The largest bending strength and least amount of wear were obtained for tile specimens firing at kiln temperature of 1100^{o} Moreover, when kiln temperature reached to 1150^{o}C, the floor tile specimens began to melt and foam was formed with pores produced.
6. When the amount of IBA replacement increased, the amounts of productions of $CaSiO_3$ and $Ca(Al_2Si_2O_8)$ produced from SiO_2 with CaO and Al_2O_3 It suggests that the amounts of $CaSiO_3$ and $Ca(Al_2Si_2O_8)$ increased with the increasing amount of IBA replacement may lead to a decrease on bending strength of tile specimens. Moreover, the amount of production of $MgSiO_3$ produced from SiO_2 and MgO increased with the increasing kiln temperature resulting in an increase of bending strength of floor tile specimens within the temperature of 1000-1100^{o}C.
7. NMR showed that values of Q4 after integration decreased with increasing amount of IBA replacement, confirming that IBA contained less amount of Si than clay, resulting lesser amount of silicate due to insufficient Si atom. Less amount of silicate lead to the decrease of bending strength which conformed with the results in bending strength tests.
8. Maximum replacement level of IBA was 20%, and its proper kiln temperature was 1050℃ or 1100℃. Kiln temperature above 1150℃ had a tendency to cause instability of tile shrinkage, making it difficult to meet the specification requirement.

Declarations

Acknowledgments The authors would like to kindly thank Ministry of Science and Technology (MOST), Taiwan for the financial support. We would also like to thank

Dr. Huan-Lin Luo of I-Shou University for his insightful opinions for completing this study.

Authors' contributions

Methodology and project administration by Deng-Fong Lin

Investigation and experiments were performed by Chia-Wen Chen

Analysis and visualization were performed by Chia-Wen Chen and Kuo-Liang Lin

The first draft of the manuscript was written by Kuo-Liang Lin and Show-Ing Shieh.

All the authors commented on previous versions of the manuscript.

All the authors contributed to review and editing according to reviewer's comments. All the authors read and approved the final manuscript.

Funding The work has received funding from Ministry of Science and Technology, Taiwan under grant agreement NSC 101-2221-E-214-063-MY3-1.

Data availability The datasets used and/or analyzed during the current study are available from the corresponding author on reasonable request.

Compliance with ethical standards

Competing interests The authors declare that they have no competing

interests.

Ethical approval and consent to participate Not applicable

Consent for publication Not applicable

References

Bernd W. & Carl F. S., *Utilization of sewage sludge ashes in the brick and tile industry.* Water Science and Technology, Volume 36, Issue 11, Pages 251-258, 1997.

Bijen J.M.J.M. *Manufacturing processes of artificial lightweight aggregates from fly ash.* International Journal of Cement Composites and Lightweight Concrete, Volume 8, Issue 3, Pages 191-199, August 1986

Bourtsalas, A., "Processing the problematic fine fraction of incinerator bottom ash into a raw material for manufacturing ceramics", Imperial College London, ISNI: 0000 0004 5371 9625, 2015.

R Cheeseman, S Monteiro da Rocha, C Sollars, S Bethanis & A. R Boccaccini. *Ceramic processing of incinerator bottom ash.* Waste Management, Volume 23, Issue 10, Pages 907-916, 2003.

EPA 2020. Management Regulations Announced for the Reuse of Incinerator Bottom Ash, Environmental Protection Administration, ROC (Taiwan). 2020.

He, Yong-Jia, and Hu, Shu-Guang, Application of ^{29}Si Nuclear Magnetic Resonance (NMR) in Research of Cement Chemistry. Journal of Material Science & Engineering, pp.147~153, Vol 25.No.1, Feb, 2007.

Schabbach, L.M., Andreola, F., Barbieri, L.,, Lancellotti, I., Karamanova, E., Karamanov A. Post-treated incinerator bottom ash as alternative raw material for ceramic manufacturing, Journal of the European Ceramic Society Volume 32, Issue 11, August 2012, Pages 2843-2852.

Lin, W. Y., Heng, K. S., Sun, X., and Wang, J. Y., “Accelerated carbonation of different size fractions of MSW IBA and the effect on leaching”, Waste Management, Vol. 41, pp. 75-84, July 1, 2015.

Mohammad Balapour, Weijin Zhao, E.J. Garboczi, Nay Ye Oo, Sabrina Spatari, Y. Grace Hsuan, Pieter Billen, Yaghoob Farnam, Potential use of lightweight aggregate (LWA) produced from bottom coal ash for internal curing of concrete systems, Cement and Concrete Composites, Volume 105, 2020, 103428, ISSN 0958-9465, https://doi.org/10.1016/j.cemconcomp.2019.103428.

Niall Holmes, Hugh O'Malley, Paul Cribbin, Henry Mullen, Garrett Keane, Performance of masonry blocks containing different proportions of incinerator bottom ash, Sustainable Materials and Technologies, Volume 8, 2016, Pages 14-19, ISSN 2214-9937, https://doi.org/10.1016/j.susmat.2016.05.001. (http://www.sciencedirect.com/science/article/pii/S2214993715300117)

P Filipponi, A Polettini, R Pomi, P Sirini, Physical and mechanical properties of cement-based products containing incineration bottom ash, Waste Management, Volume 23, Issue 2, 2003, Pages 145-156, ISSN 0956-053X, https://doi.org/10.1016/S0956-053X(02)00041-7.

Ranguelov, A. Karamanov, Post-treated incinerator bottom ash as alternative raw material for ceramic manufacturing, Journal of the European Ceramic Society, Volume 32, Issue 11, 2012, Pages 2843-2852, ISSN 0955-2219, ttps://doi.org/10.1016/j.jeurceramsoc.2012.01.020. (http://www.sciencedirect.com/science/article/pii/S0955221912000349)

Valle-Zermeño, R., Barreneche, C., Cabeza, L. F., Formosa, J., Fernández, A. I., and Chimenos, J. M., “MSWI bottom ash for thermal energy storage: An innovative and sustainable approach for its reutilization”, Renewable Energy, Vol. 99, pp. 431-436, December 1, 2016.

Figures

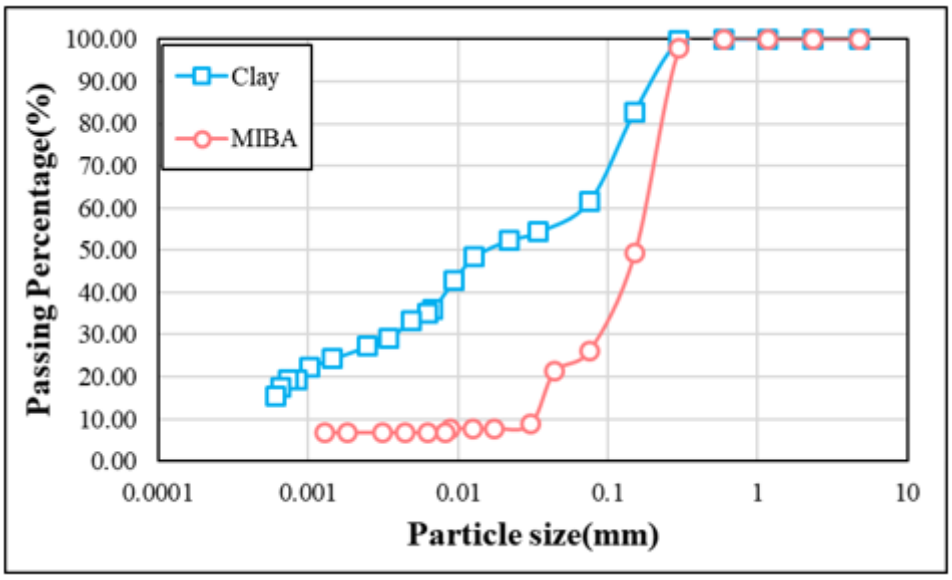

Figure 1

Particle size distributions for clay and IBA

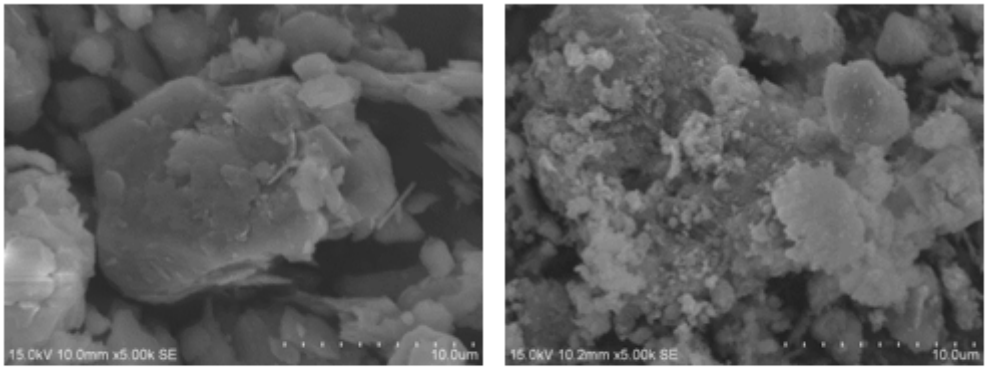

(a)clay (b)bottom ash

Figure 2

SEM of the raw materials

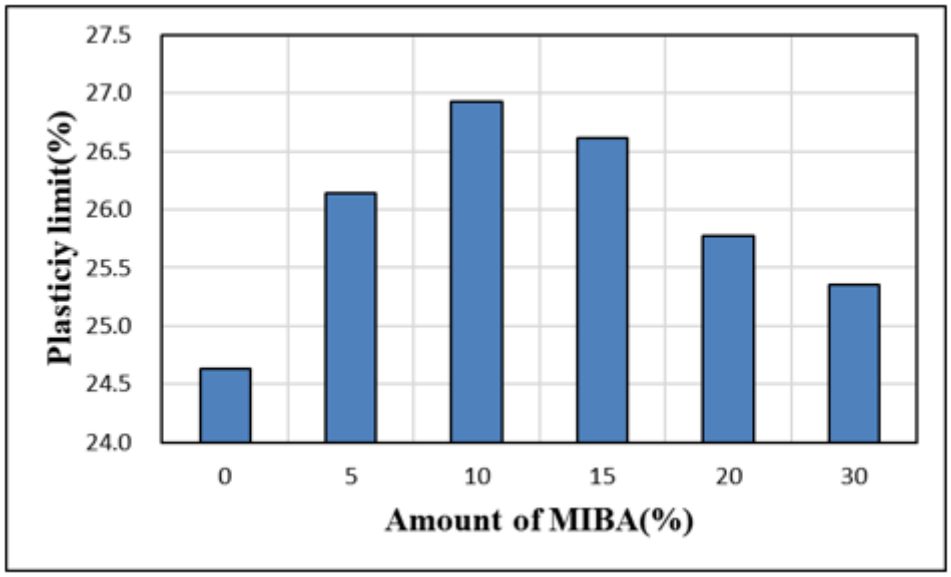

Figure 3

Atterberg limits

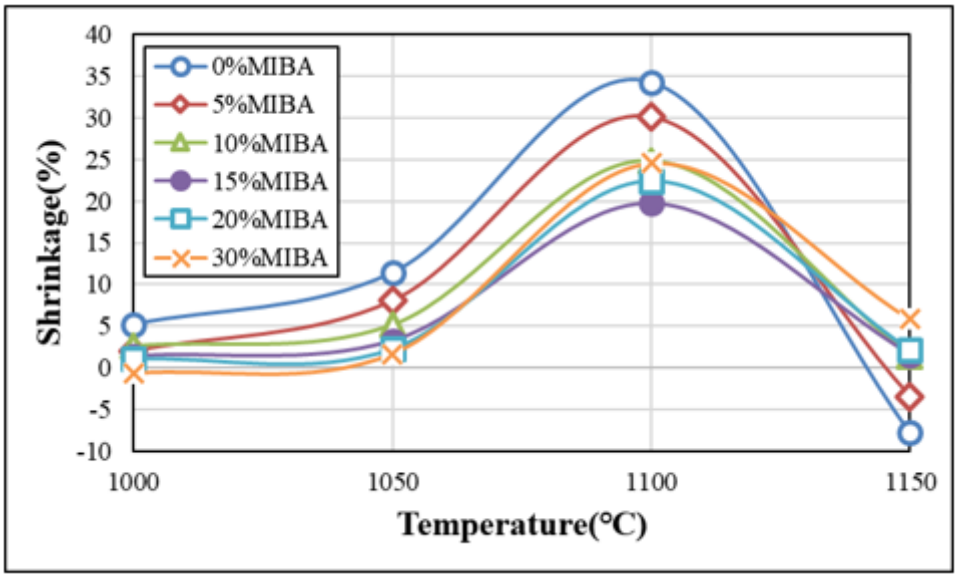

Figure 4

Shrinkage for floor tile specimens

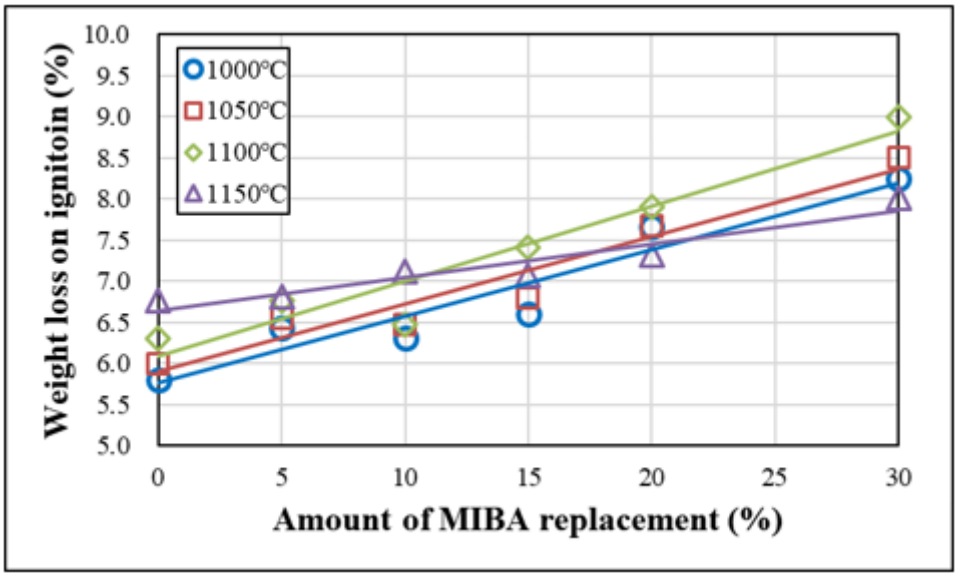

Figure 5

Weight loss on ignition for floor tiles

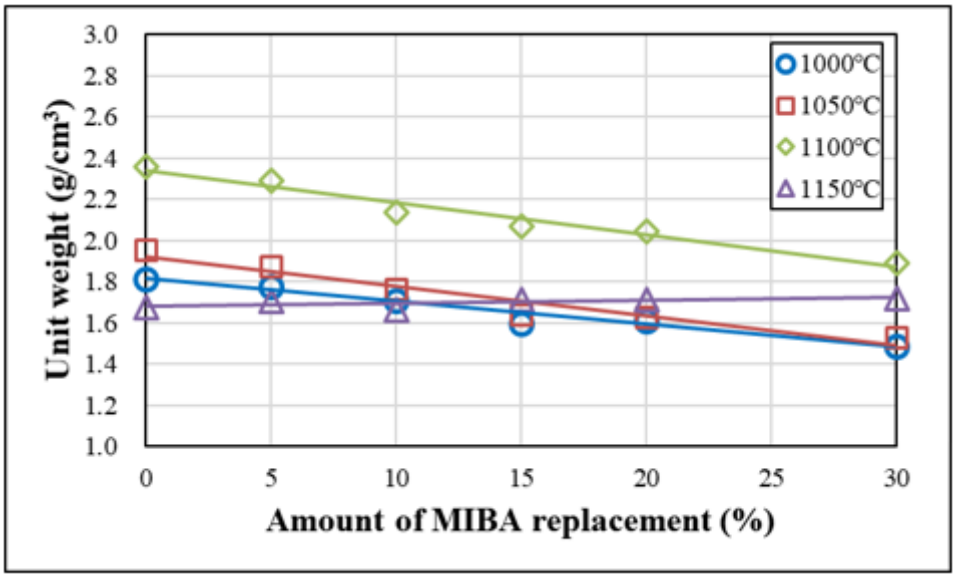

Figure 6

Specific gravity for floor tiles

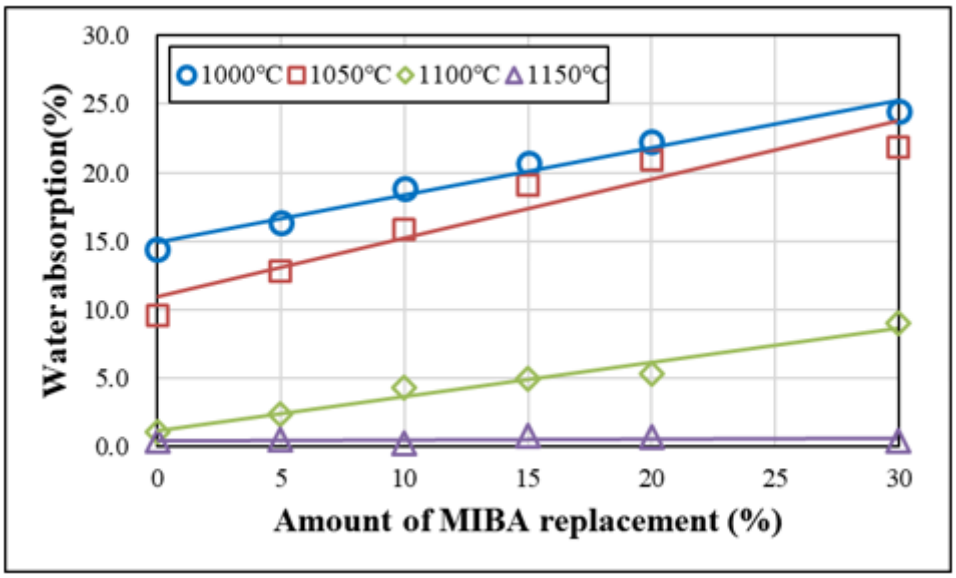

Figure 7

Water absorption for floor tiles

Figure 8

Tile specimen kilned at 1150°C

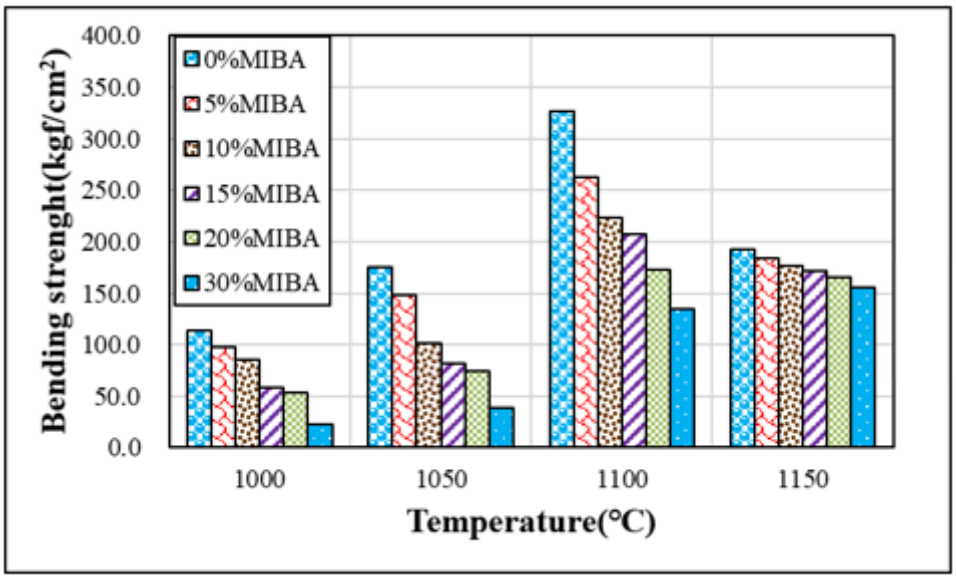

Figure 9

Bending strength for floor tiles

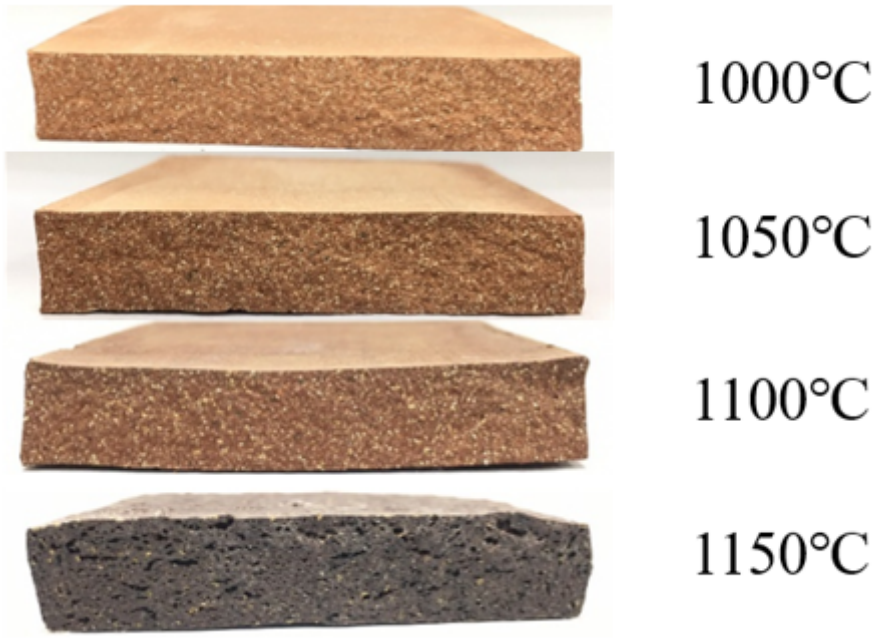

Figure 10

Cross sections with 20% IBA replacement at different kiln temperatures

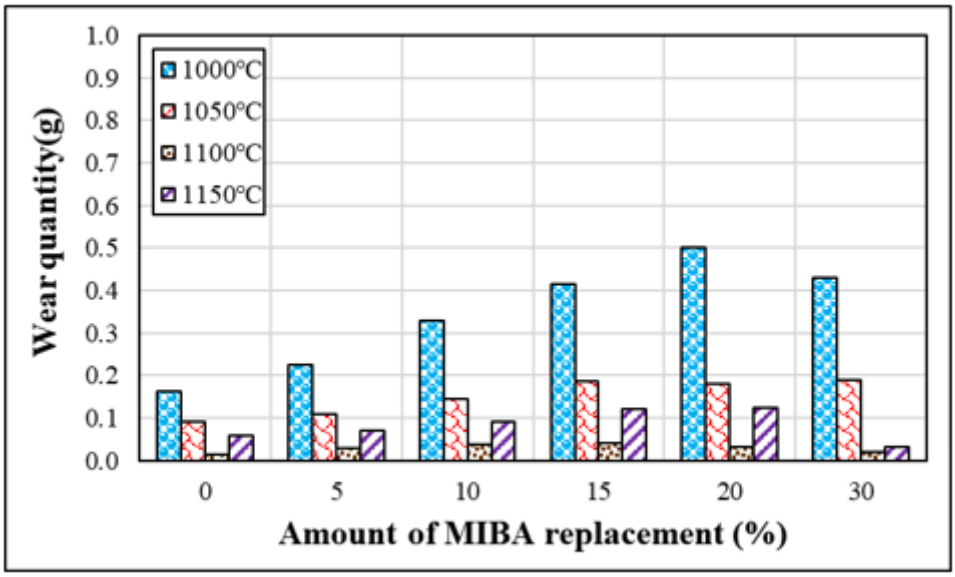

Figure 11

Wear resistance for floor tiles

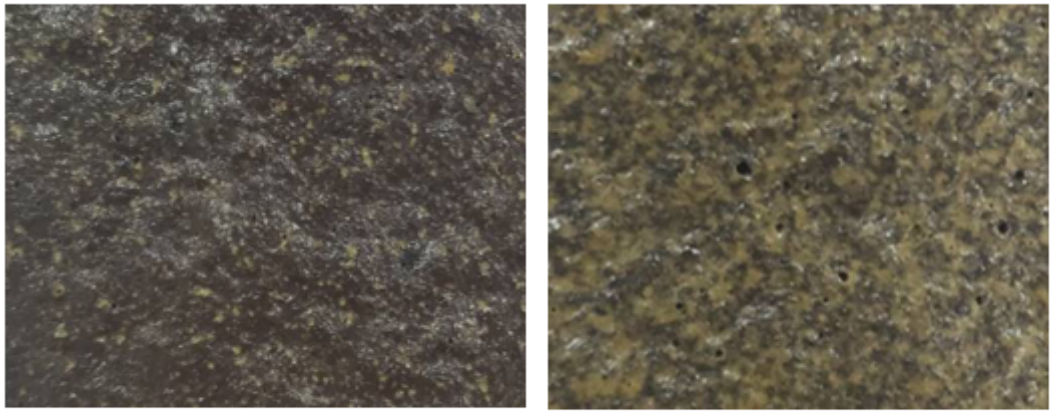

(a) 20% IBA replavement (b) 30%IBA replacement

Figure 12

Surface wear spotted at 20% and 30% replacement

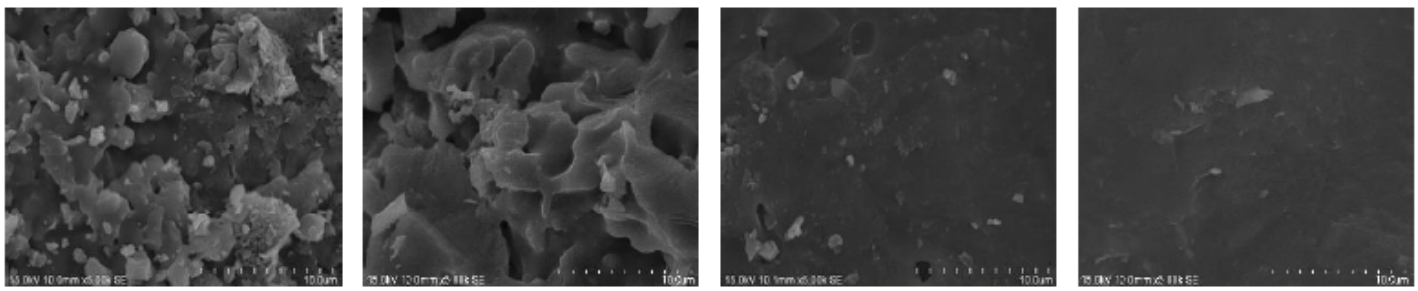

(a)1000°C (b)1050°C (c)1100°C (d)1150°C

Figure 13

SEM with increasing temperature with 0% IBA replacement

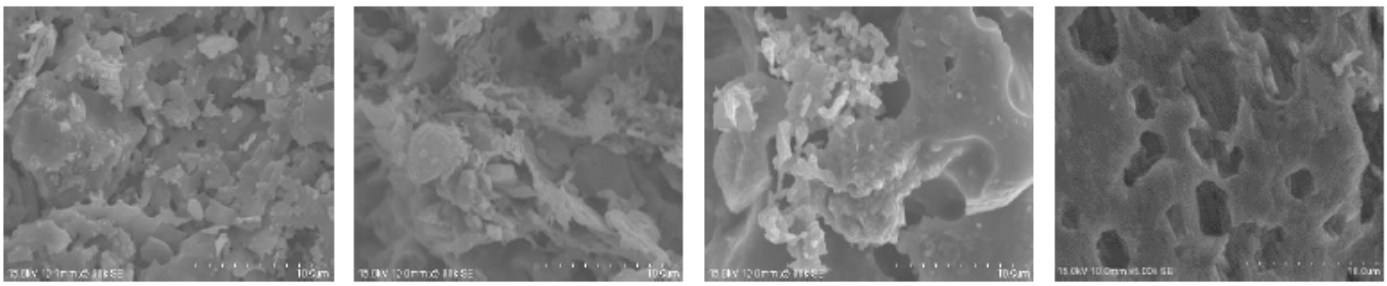

(a)1000°C (b)1050°C (c)1100°C (d)1150°C

Figure 14

SEM with increasing temperature with 20% IBA replacement

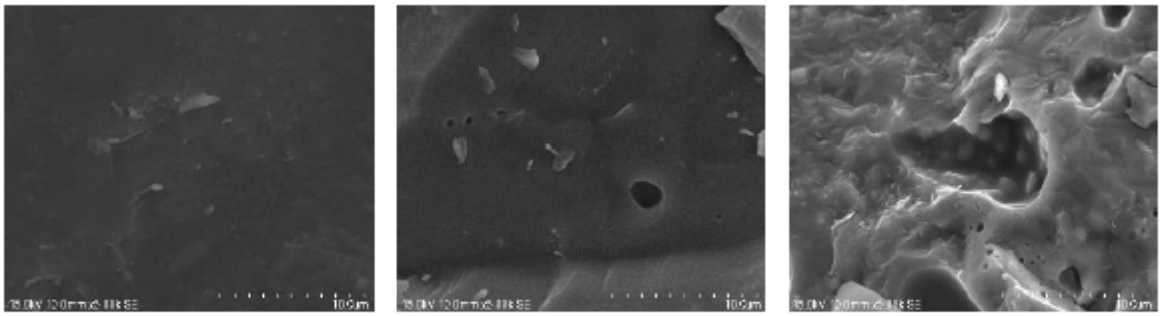

(a) 5% IBA (b)10% IBA (c) 15%IBA

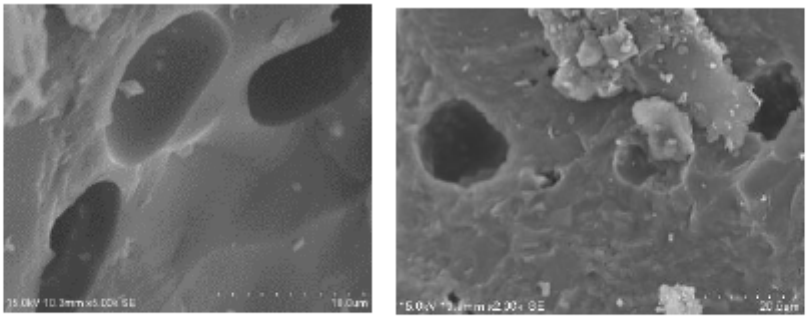

(d) 20%IBA (e) 30% IBA

Figure 15

SEM with increasing IBA replacement at 1150°C

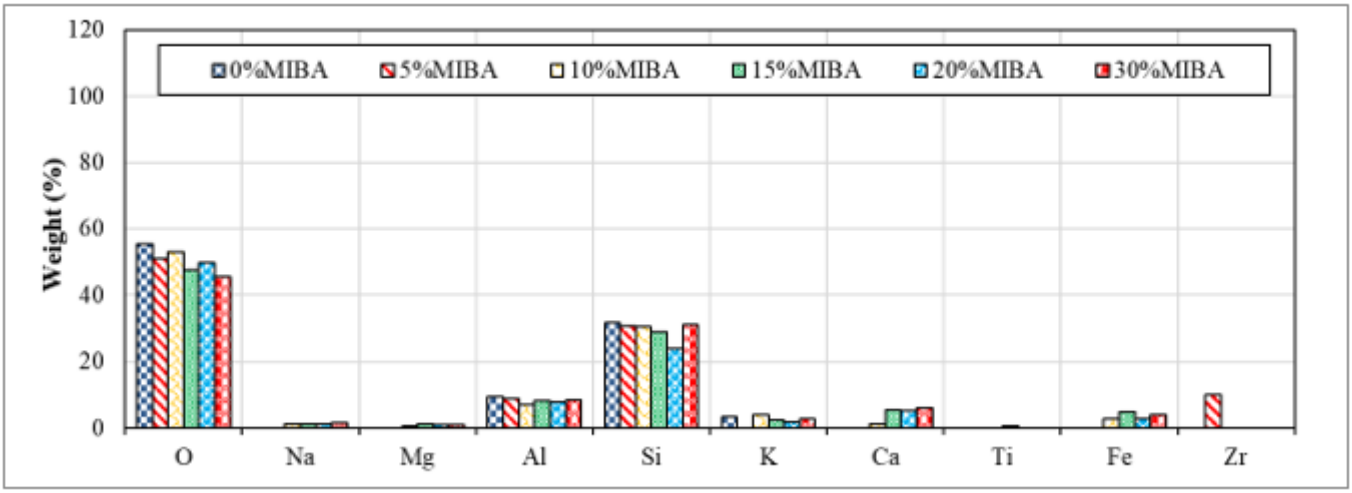

Figure 16

EDS analysis for floor tiles

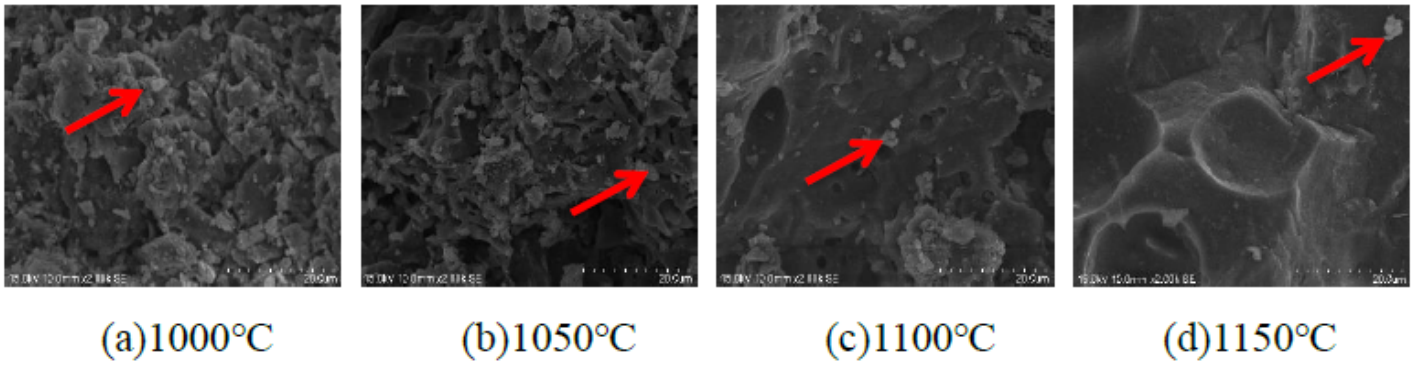

Figure 17

SEM of 0% IBA replacement with increasing kiln temperature

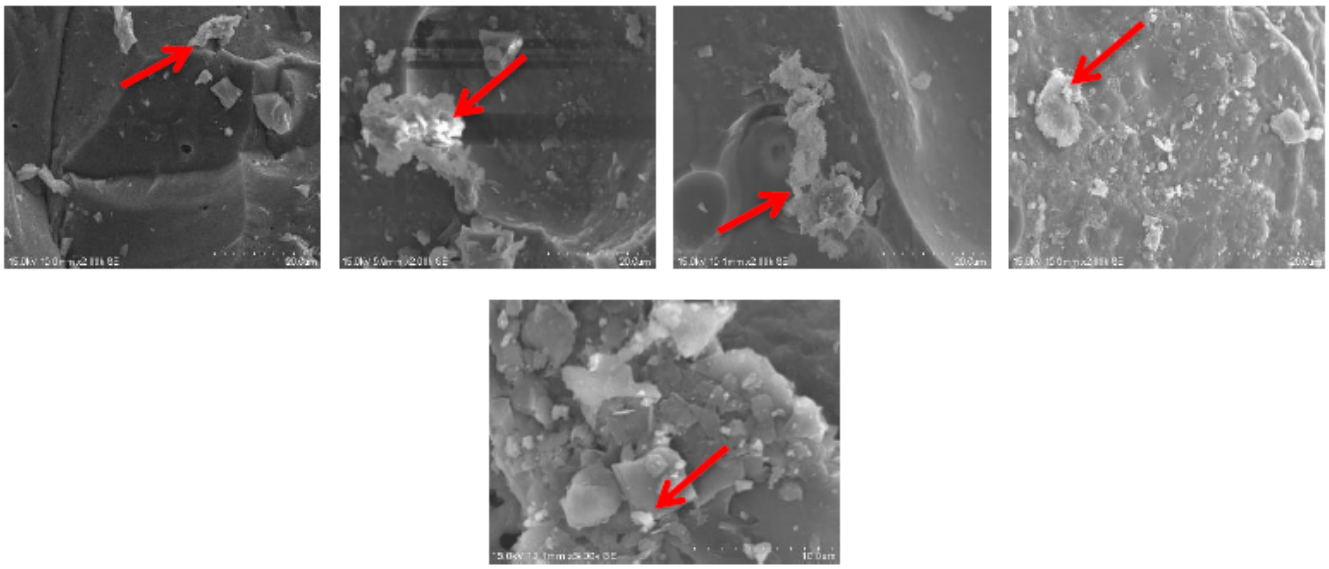

(a)5% (b)10% (c)15% (d)20% (e)30%

Figure 18

SEM of different % IBA replacement at 1150°C kiln temperature

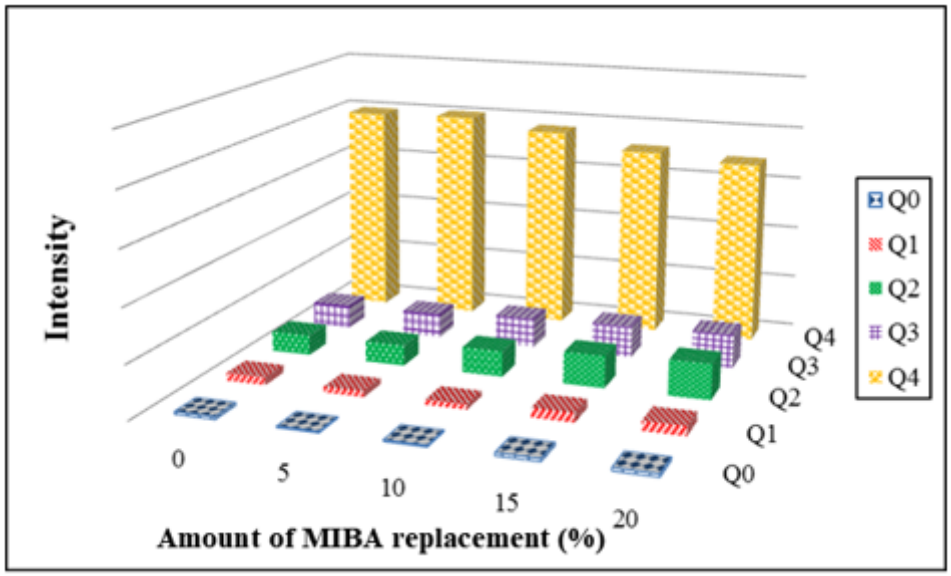

Figure 19

Si-NMR of 0~20% IBA replacement at 1050°C kiln temperature